ELSEVIER

Biophysical Chemistry 101–102 (2002) 347–358

Biophysical Chemistry

www.elsevier.com/locate/bpc

Listeria monocytogenes phosphatidylinositol-specific phospholipase C: activation and allostery

Margret Ryan[a], Tatiana O. Zaikova[b], John F.W. Keana[b], Howard Goldfine[c], O. Hayes Griffith[a,b,*]

[a]*Institute of Molecular Biology, University of Oregon, Eugene, OR 97403-1253, USA*
[b]*Department of Chemistry, University of Oregon, Eugene, OR 97403-1253, USA*
[c]*Department of Microbiology, School of Medicine, University of Pennsylvania, Philadelphia, PA 19104-6076, USA*

Received 15 March 2002; received in revised form 22 April 2002; accepted 22 April 2002

Abstract

The animal and human pathogen *Listeria monocytogenes* secretes several virulence factors, including a phosphatidylinositol-specific phospholipase C (PI-PLC). Sufficient quantities of *L. monocytogenes* PI-PLC for biophysical studies were obtained by overexpression of the enzyme in *Escherichia coli*. The purified PI-PLC was examined in enzyme kinetics experiments using a new fluorogenic substrate, methyl-FLIP. Methyl-FLIP is a water-soluble monomeric substrate cleaved in a manner similar to the natural aggregate substrate, phosphatidylinositol (PI). Michaelis–Menten kinetics were observed with $K_M = 61 \pm 7$ μM and $V_{max} = 120 \pm 5$ μmol min^{-1} mg^{-1}, corresponding to $k_{cat} = 66 \pm 3$ s^{-1}. The catalysis is activated by the addition of a short-chain phospholipid, dihexanoyl phosphatidylcholine (diC_6PC). The kinetics were fitted to a two-site model in which the substrate binds to the active site and diC_6PC binds to a second site, with an interaction between the two sites. The result is a decrease in K_M and an increase in V_{max}, producing an overall four to five-fold increase in catalytic efficiency (k_{cat}/K_M). The interaction is not a regulatory mechanism, as is the case for multimeric enzymes; rather, it suggests interfacial cooperativity between the active site and a lipid-binding subsite, presumably adjacent to the active site.

Keywords: Enzyme kinetics; Interfacial activation; Phosphatidylinositol-specific phospholipase C (PI-PLC); Co-operativity

1. Introduction

Listeria monocytogenes is a Gram-positive, non-spore-forming bacterium. It can be found in soil, decaying plants and food, and causes listeriosis in animals and humans. The pathogen is most often acquired by consumption of food contaminated with live bacteria. Listeriosis is a serious infection in pregnant women and their fetuses and neonates, and is also a disease of the elderly and immunocompromised individuals [1]. There are approximately 2500 annual cases of severe listeriosis in the US with a 20% mortality rate [2]. Following entry through the gut, the bacterium induces its own uptake into a variety of cells and is actively taken up by professional phagocytes. *L. monocy-*

*Corresponding author. Tel.: +1-541-346-4634; fax: +1-541-346-5891.
E-mail address: hayes@molbio.uoregon.edu (O.H. Griffith).

0301-4622/02/$ - see front matter © 2002 Elsevier Science B.V. All rights reserved.
PII: S0301-4622(02)00158-8

togenes escapes from the phagosome into the cytosol and multiplies. It recruits actin filaments to induce movement through the cytosol, and to form a pseudopod-like structure with a bacterium at the tip, which is then internalized into neighboring cells. Through the blood stream the bacteria are distributed to different organs. *L. monocytogenes* secretes a number of virulence factors to facilitate crossing the multiple membrane barriers. One of these, listeriolysin O, a pore-forming toxin, is essential for escape of the bacteria from the phagosomal compartment in the mouse model of infection [3]. *L. monocytogenes* also secretes two phospholipases, a phosphatidylinositol-specific phospholipase C (PI-PLC) and a broad-range phospholipase C (PC-PLC) [3]. A double mutant lacking both phospholipases was 500-fold less virulent in mice and exhibited diminished ability to escape from the primary vacuole and to spread to other cells [4]. The focus in this study is on the PI-PLC. The PI-PLC gene is part of the virulence gene cluster of *L. monocytogenes* [5]. The loss of PI-PLC by either deletion or site-specific mutation results in diminished escape from the primary vacuole of macrophages [6,7]. PI-PLCs are secreted by a number of other Gram-positive bacteria, including the pathogens *Bacillus cereus*, *B. thuringiensis*, *B. anthracis*, *L. ivanovii*, *Staphylococcus aureus*, *Clostridium novyi* and *Rhodococcus equii*. The best-studied bacterial isozymes are the *B. cereus* and the essentially identical *B. thuringiensis* PI-PLCs (for a review see [8]). The crystal structures of two bacterial enzymes have been solved, *B. cereus* PI-PLC [9,10] and *L. monocytogenes* PI-PLC [11]. The bacterial enzymes are small, 33–36 kDa, and consist of a single domain that is remarkably similar to the catalytic domain of the complex and highly regulated second messenger-producing PI-PLC δ1 of eukaryotic cells [12,13]. We report here the first enzyme kinetics study of *L. monocytogenes* PI-PLC utilizing a novel fluorogenic substrate, methyl-FLIP that we have recently synthesized [14]. PI-PLC cleaves this water-soluble and non-fluorescent substrate as it does the natural substrate, PI (Fig. 1). Cleavage of methyl-FLIP produces a highly fluorescent product that can be readily monitored.

2. Experimental

2.1. Materials and general techniques

Plasmid DNA was prepared using the Wizard Plus SV Minipreps kit (Promega, Madison, WI).

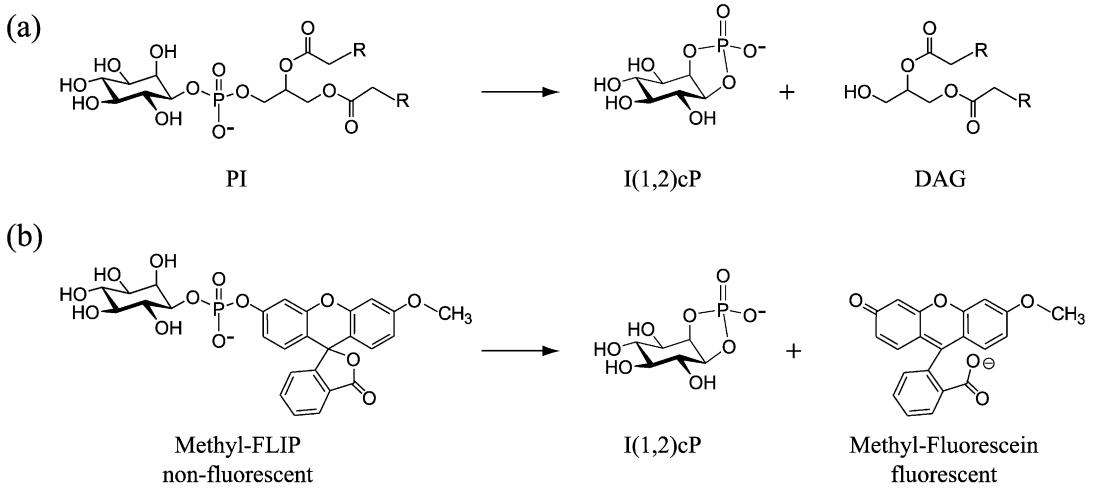

Fig. 1. Bacterial PI-PLCs cleave the fluorogenic substrate methyl-FLIP in an intramolecular phosphotransferase reaction similar to the cleavage of the natural substrate. (a) The natural substrate phosphatidylinositol (PI) is cleaved by PI-PLC, forming *myo*-inositol 1,2-cyclic phosphate [I(1,2)cP] and *sn*-1,2-diacylglycerol (DAG). (b) In an analogous manner, PI-PLC cleaves the non-fluorescent water-soluble substrate methyl-FLIP to form I(1,2)cP and a fluorescein derivative that is highly fluorescent. R, hydrocarbon chain.

Synthetic oligonucleotides were obtained Econo-PURE from BioSource International Inc (Camarillo, CA) and used without further purification. All polymerase chain reactions (PCRs) were carried out using 3′–5′ proofreading Pwo DNA polymerase, buffer and nucleotides from Roche Molecular Biochemicals (Indianapolis, IN) in a 50-μl reaction volume and an MJ Research DNA Engine PTC-200 thermocycler. PCR products were purified by recovery from low-melting agarose gels (QIAquick Gel Extraction Kit, Qiagen Inc, Valencia, CA). Restriction endonucleases were from Roche and Promega, and T4 DNA ligase from New England Biolabs (Beverly, MA). Competent *Escherichia coli* MM294 cells were transformed using TSS solution (Epicentre Technologies, Madison, WI). DNA sequencing was carried out on an ABI PRIZM 377 DNA Sequencer (PE Applied Biosystems, Foster City, CA) at the DNA Sequencing Facility (Institute of Molecular Biology, University of Oregon). N-terminal amino acid sequence was determined at the University of Oregon Biotechnology Laboratory by Edman degradation on a Model 470A liquid-phase protein sequencer with a Model 120 PTH Analyzer (PE Applied Biosystems). S-Sepharose FF and low-substitution Phenyl Sepharose FF column media (Pharmacia, Piscataway, NJ) were used as recommended by the manufacturer. Bovine liver PI, sodium salt, was from Avanti Polar Lipids (Alabaster, AL), [^{3}H]PI from Perkin Elmer Life Sciences Inc (Boston, MA) and *B. cereus* PI-PLC from Molecular Probes (Eugene, OR). Other chemicals were from the following manufacturers: sodium deoxycholate and the free acid form of HEPES and MES (Calbiochem, San Diego, CA), bovine skin Type B gelatin at 225 Bloom, chicken egg white lysozyme and Tris base (Sigma, St. Louis, MO), BSA (USB Corp, Cleveland, OH). Deionized water of >17.5 MΩ cm was used throughout.

2.2. Plasmid constructs

The plasmid for overexpression of *B. cereus* PI-PLC, pHS475 [15,16], was adapted for expressing different genes of interest in the same manner. A blunt end restriction site, NaeI, was introduced directly between the coding regions of the STII signal for periplasmic expression and the amino terminus of PI-PLC. This modification was constructed by two-step PCR. The first PCR product was generated from a forward-flanking primer upstream of a BamHI site and the STII signal sequence, and the reverse primer 5′-GCTgcCg-GCATAGGCATTTG for the generation of the NaeI site (underlined) by conservatively changing three nucleotides (lower case). In the second step, the purified product of the first reaction was used as the forward primer together with a reverse primer located 3′ of a HindIII site internal to the *B. cereus* PI-PLC gene. Digestion with *Bam*HI and *Hin*dIII produced a 543-bp fragment, which was ligated into pHS475 after removal of the resident corresponding fragment and all extra *B. cereus* sequence, which is flanked at the 3′ end by additional HindIII sites. The resulting vector, pHSNae1, contains a 448-bp NaeI–HindIII stuffer fragment. The integrity of the regions manipulated by PCR was confirmed by DNA sequencing.

The *L. monocytogenes* PI-PLC precursor gene was obtained from pEJ7, kindly provided by Hao Shen, University of Pennsylvania. pEJ7 resulted from the cloning in pBR322 of a 1886-bp EcoRI fragment from *L. monocytogenes* (derived from a 3550-bp genomic fragment, GenBank accession number M24199). For cloning into pHSNae1 a forward PCR primer was designed, starting at the codon for amino acid 23 of the precursor: 5′-TTCCCATTAGGCGGAAAAG. The reverse primer, 5′-CTTCAAGAATTCTTCTGCTTGAG, contained the original EcoRI (underlined) site downstream of the PI-PLC gene. pHSNae1 was digested at an EcoRI site internal to the stuffer fragment and the NaeI site. The amplified region was ligated to the vector fragment and the resulting construct, pHSEJ7, transformed into *E. coli* MM294. The nucleotide sequence of the entire insert was confirmed. A vector similar to pHSNae1 [16], but lacking the Nae1 site, had been previously used to clone and overexpress *L. monocytogenes* PI-PLC for its crystal structure determination. In this case, the cloned fragment starts with amino acid 30 of the PI-PLC precursor and an incorrect residue was incorporated at the N-terminus, Ser instead of Tyr, as a result of the cloning strategy [11].

2.3. Enzyme expression and purification

The *L. monocytogenes* PI-PLC was expressed in *E. coli* MM294 from pHSEJ7 in a 1-l culture volume as previously described for the expression of *B. cereus* PI-PLC [16]. Release from the periplasmic space by lysozyme and mild osmotic shock treatment was essentially as reported [17], except that Tris–HCl, pH 7.3, was used. The resulting 200 ml of solution of periplasmic proteins in 0.1 M Tris–HCl, pH 7.3, 0.5 M sucrose, 20 mM $MgCl_2$, 0.5 mM EDTA, 0.03 mg/ml lysozyme was diluted with 800 ml of 50 mM NaCl and dialyzed against 8 l of 20 mM MES, pH 6.5, 50 mM NaCl, 4 mM $MgCl_2$ using a Hollow Fiber Bundle, MWCO 18 000 (Spectrum Laboratories, Rancho Dominguez, CA). The material was then separated on an S-Sepharose FF column using a 0.05–1.05 M NaCl gradient in dialysis buffer. The peak activity fractions were concentrated, diluted 1:50 in 1.5 M $(NH_4)_2SO_4$, 50 mM HEPES, pH 7.2, applied to a Phenyl Sepharose column and eluted using a 1.5–0 M $(NH_4)_2SO_4$ gradient in 50 mM HEPES, pH 7.2. All purification steps were carried out at 4 °C. The PI-PLC recovered is approximately 90% pure, as judged from Coomassie-stained SDS-PAGE gels, and was stored at −20 °C. Approximately 5 mg of purified PI-PLC was obtained from a 1-l culture. Amino acid sequencing of six residues of the N-terminus revealed that the mature protein starts at residue 30. The concentration of purified, mature protein (288 residues, MW 32 900) was determined by absorbance at 280 nm using a calculated molar extinction coefficient of 32 430 [18].

2.4. Mixed micelle enzyme assay

This assay uses detergent-solubilized [^{3}H]PI substrate essentially as described [19], with some modifications. The enzyme was diluted in 0.1% BSA, 50 mM HEPES, pH 7.2, 20 mM $MgCl_2$ to a concentration of approximately 32 pM. A 100-μl assay was prepared by combining, in the following order: 6 μl of [^{3}H]PI in deoxycholate (this suspension was prepared by mixing 1 μl of 10 mM [^{3}H]PI in H_2O, specific activity ~500 000 cpm/μmol, and 5 μl of 1% deoxycholate); 5 μl of 1% deoxycholate; 40 μl of 0.1 M HEPES, pH 7.2; 29 μl of H_2O; and 20 μl of diluted enzyme to start the reaction. Reactions were maintained in a 37 °C water bath for 20 min, then extracted with 5 volumes of chloroform/methanol/HCl (66:33:1). The water-soluble reaction products contained in the aqueous phase were quantitated by scintillation counting. *B. cereus* PI-PLC was assayed under the same conditions, except that $MgCl_2$ was omitted from the enzyme dilution buffer. Less than 20% of substrate was converted to product during the reactions, assuring linearity of substrate turnover with time.

2.5. Fluorogenic enzyme assay

This assay uses the water-soluble fluorogenic substrate methyl-FLIP. The preparation of methyl-FLIP has been previously described [14]. A 10.4 mM methyl-FLIP stock solution was prepared in H_2O and stored at −20 °C. When diC_6PC was present in the reaction, it was added from an approximately 5 mM stock solution freshly prepared in 50 mM HEPES, pH 7, and 0.1 M NaCl. Exact concentrations of solutions of methyl-FLIP substrate and diC_6PC were determined by phosphate analysis using digestion with $H_2O/H_2SO_4/HClO_4$ (18.6:1:0.4) to release inorganic phosphate, followed by color development with ammonium molybdate and sodium ascorbate [20]. The enzyme was diluted in 0.05% gelatin, 20 mM HEPES, pH 7.2, 1 M $(NH_4)_2SO_4$ and 1 mM EDTA to a concentration of 2.23 or 4.47 nM. A 0.8-ml assay volume contained varying amounts of substrate or substrate and diC_6PC in final concentrations of 50 mM HEPES, pH 7, and 0.1 M NaCl, with 5 μl of diluted enzyme added last. The fluorescence was then recorded for 3 min. Background spectra were recorded for these reactions prior to the addition of enzyme to correct for decomposition of substrate in the absence of enzyme. This rate is small; approximately 0.0013% of the racemic substrate decomposes in 3 min. Fluorescence spectra were recorded on a Hitachi F-4500 fluorescence spectrophotometer (Hitachi Instruments Inc, San Jose, CA) thermostatted at 25 °C and fitted with a yellow cut-off filter (Y-50, Hoya Corp USA, San Jose, CA) on the emission side. All spectra were

recorded using excitation and emission wavelengths of 465 and 520 nm, respectively, and a slit width of 10 nm. Methacrylate cuvets (4.5-ml capacity, 10-mm path length) were used throughout. To convert fluorescence to product concentration, a standard curve was generated from fluorescence measurements of several different product concentrations under the conditions of the assays. The linear relationship shows 9948 fluorescence units per 1 μM product.

2.6. Treatment of kinetic data

The initial reaction rate was determined by fitting of the data by linear regression or a first-order rate equation. Values for K_M and V_{max} were determined using the Michaelis–Menten equation. Fitting of the data was carried out by least-squares methods using GRAFIT (Erithacus Software Limited, Horley, UK). Parameters for the two-site model were obtained using MATHCAD (MathSoft, Cambridge, MA).

3. Results

3.1. Cloning and expression

The cloning of *L. monocytogenes* PI-PLC into pHSNae1 resulting in pHSEJ7 allowed us to verify that the mature PI-PLC starts with amino acid 30 of the PI-PLC precursor, and to produce sufficient amounts of protein for kinetic studies. The PI-PLC precursor contains a signal sequence for secretion, the length of which was predicted to be at least 22 amino acids [21]. In pHSEJ7, the *L. monocytogenes* sequence inserted starts at amino acid 23 of the PI-PLC precursor. Determination of the amino acid sequence of the N-terminus of the expressed protein showed that the predicted possible cleavage site for the signal sequence of the PI-PLC precursor, after amino acid 22, is not a valid one. Instead, the amino acid sequence verified that the mature protein starts at residue 30, in agreement with previous results [22] for the native enzyme isolated from *L. monocytogenes* culture medium and results using the program SIGNALP V1.1 [23] for the prediction of signal cleavage sites (Fig. 2). This means that the *L. monocytogenes* signal peptide is recognized in *E. coli* as well, where it is present in a truncated form of seven C-terminal residues that are fused to the *E. coli* STII signal peptide.

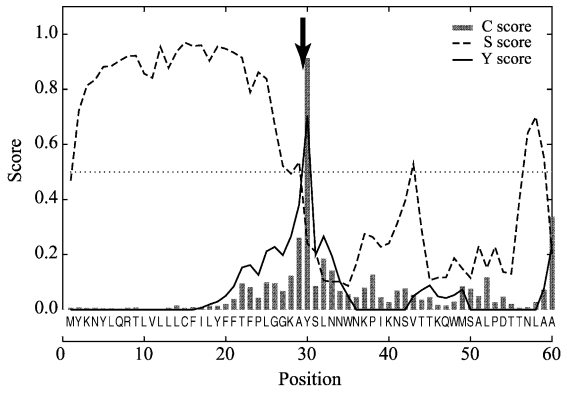

Fig. 2. Prediction of the *L. monocytogenes* PI-PLC precursor signal peptide cleavage site. The N-terminal 60 amino acid residues of the precursor protein were input into the program SIGNALP (http://www.cbs.dtu.dk/services/SignalP/). The C-score, or raw cleavage site score, is high at position #1 immediately after the cleavage site, and the S-score, or signal peptide score, is high at all residues before the cleavage site. The Y-score, or combined cleavage site score, is derived from the C- and S-scores and is high for the first amino acid of the predicted mature protein. An arrow indicates the predicted cleavage site.

3.2. Mixed micelle assay

The activity of recombinant *L. monocytogenes* PI-PLC was compared to activity data for the native enzyme and *B. cereus* PI-PLC. The activity of bacterial PI-PLCs is most commonly measured in a mixed micelle assay with the natural substrate PI dispersed in detergent. In the presence of 0.1 mM PI and 0.1% deoxycholate in 50 mM HEPES, pH 7.2, the specific activity ranges from 700 to 1300 μmol min^{-1} mg^{-1} for *L. monocytogenes* PI-PLC when the enzyme added to the assay was diluted in 0.1% BSA, 50 mM HEPES, pH 7.2, and 20 mM $MgCl_2$. This results in a final concentration of 4 mM $MgCl_2$ in the assay. In the absence of added $MgCl_2$, the activity measures only approximately 30 μmol min^{-1} mg^{-1}. The activity-enhancing effect of salt has been noted before and is described in detail for this enzyme expressed in

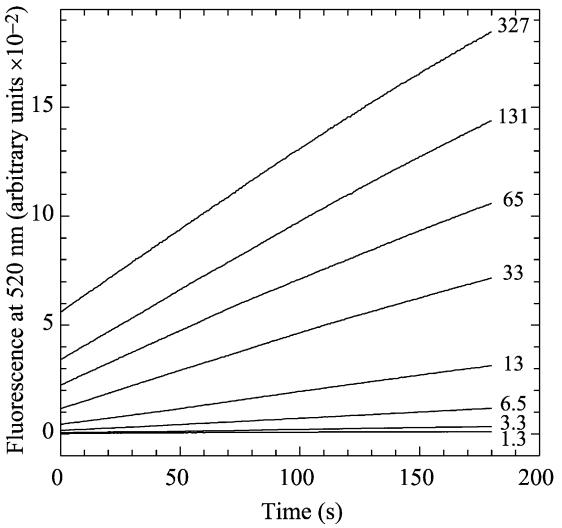

Fig. 3. Time course of methyl-FLIP turnover by *L. monocytogenes* PI-PLC as measured by methyl-fluorescein product generation. The turnover of methyl-FLIP substrate, 1.3–327 μM as indicated at the end of each line, is measured as increased fluorescence emission at 520 nm (with excitation at 465 nm). The lines are continuous data sets from the spectrometer output. The fluorescence vs. time response was used to obtain the initial rate by fitting to a first-order rate equation or, for low substrate concentrations, by linear regression. This is a representative subset of the data used to calculate V_{max} and K_M shown in Fig. 4. Enzyme concentration for all data sets was 14 pM.

L. monocytogenes DP-L1470 as a non-specific effect that can also be achieved with $(NH_4)_2SO_4$ or KCl, but at higher concentrations of approximately 0.1 or 0.3 M [22]. For comparison, *B. cereus* PI-PLC activity is 1300–1900 μmol min^{-1} mg^{-1}, measured under the same conditions as the *L. monocytogenes* enzyme, but without added salt. The effect of divalent or monovalent cations on *B. cereus* PI-PLC is the opposite of the effect on *L. monocytogenes* PI-PLC, e.g. it has been reported that ~0.2 mM NaCl reduces the activity of the *B. cereus* enzyme by 50% [24].

3.3. Enzyme kinetics with methyl-FLIP

The initial rates of cleavage of methyl-FLIP were determined by measuring the fluorescence of the product as a function of time. Fig. 3 shows an initial linear period during the appearance of fluorescence with time and an increase in fluorescence with substrate concentration, as expected for a well-behaved enzyme kinetics system. The substrate, methyl-FLIP, is a pure compound. However, as synthesized it is a 50:50 mixture (a racemic mixture) of the D- and L-enantiomers. The concentrations given in Fig. 3, and throughout this paper, refer to that of the active D-enantiomer, i.e. one-half of the concentration of racemic substrate. It has previously been shown that the L-enantiomers of both the chromogenic substrate *myo*-inositol 1-(4-nitrophenyl phosphate) [25] and a short-chain PI [26] are neither substrates nor inhibitors in the kinetics of the closely related bacterial PI-PLCs from *B. cereus* and *B. thuringiensis*, respectively. The active sites of bacterial PI-PLCs are highly stereospecific, and only the D-enantiomer binds and is cleaved.

The initial rates as a function of substrate concentration (Fig. 4) can be fitted to a rectangular hyperbola, and thus obey standard Michaelis–Menten kinetics. The non-linear regression analysis yields $K_M = 61 \pm 7$ μM and $V_{max} = 120 \pm 5$ μmol

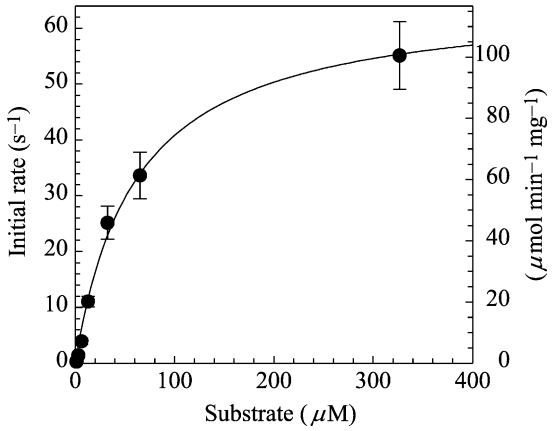

Fig. 4. *L. monocytogenes* PI-PLC catalysis of methyl-FLIP follows Michaelis–Menten kinetics. Each data point represents the mean (±S.D.) of two–four measurements of the initial rate. The solid line is the fitted curve with $V_{max} = 66$ s^{-1} and $K_M = 61$ μM. Two common scales are shown on the *y*-axis. The scale on the left is in μmol product s^{-1} $μmol^{-1}$ enzyme (abbreviated s^{-1}), and on the right the scale is μmol product min^{-1} mg^{-1} enzyme (abbreviated μmol min^{-1} mg^{-1}). The same conventions are used in the following figures. The *L. monocytogenes* PI-PLC concentration was 14 pM.

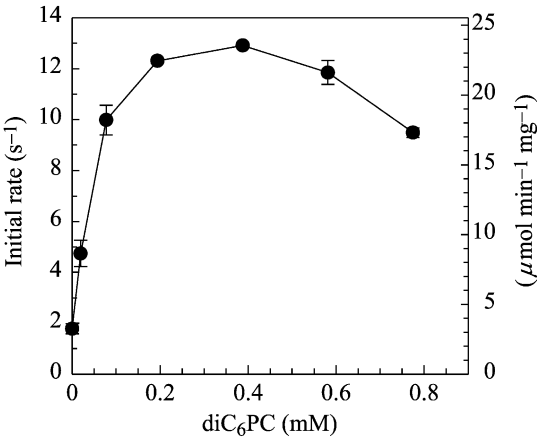

Fig. 5. The short-chain phosphatidylcholine diC$_6$PC activates *L. monocytogenes* PI-PLC. Increasing concentrations of the neutral diC$_6$PC lead to an increased turnover of methyl-FLIP substrate with a maximum 7.2-fold increase at approximately 0.4 mM diC$_6$PC. Each data point represents the mean ($\pm$S.D.) of two measurements. Data points are connected by a straight line. The enzyme and substrate concentrations were held constant at 28 pM and 3.25 μM, respectively.

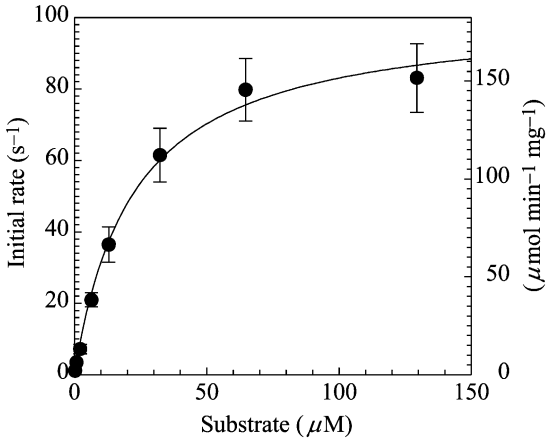

Fig. 6. Dependence of the initial rate of *L. monocytogenes* PI-PLC catalysis on substrate concentration in the presence of a fixed concentration (0.4 mM) of diC$_6$PC activator. The solid line is a non-linear regression fit to the data with kinetic constants of $V_{max}^{app} = 102$ s^{-1} and $K_M^{app} = 22$ μM. Each data point represents the mean ($\pm$S.D.) of two measurements and was used to obtain the fitted curve. Enzyme concentration, 14 pM.

min^{-1} mg^{-1}. Converting V_{max} to μmoles of product per second per μmoles of enzyme (abbreviated s^{-1}) by multiplying by 32.90/60 (the factor of 32.90 is the molecular weight of *L. monocytogenes* PI-PLC in kDa, and the divisor is the conversion from min to s) gives $k_{cat} = 66 \pm 3$ s^{-1}.

The catalysis is activated in the presence of a short-chain phosphatidylcholine, diC$_6$PC (Fig. 5). The plot of the initial rates steeply rises with added lipid, reaches a maximum in the region of 0.4 mM diC$_6$PC, and then decreases. A fit of the initial activation region, $0 < [\text{diC}_6\text{PC}] < 0.25$ mM, to a single binding-site model yields a value of the dissociation constant $K_d = 0.06 \pm 0.01$ mM. This method of estimating K_d requires that the substrate concentration be low, so that the ratio $[S]/K_s$ is negligible compared to other terms in the kinetic equation, and $[S]/\alpha K_s \ll 1$. In another experiment, the concentration of diC$_6$PC was fixed at 0.4 mM and the initial rates were measured as a function of substrate concentration, as for Fig. 4. The results are shown in Fig. 6. The solid line is a fit to the Michaelis–Menten equation, with $K_M^{app} = 22 \pm 3$ μM and $V_{max}^{app} = 186 \pm 7$ μmol min^{-1} mg^{-1}, equivalent to 102 ± 4 s^{-1}.

3.4. Kinetic model

To account for these data, a two-site model with a lipid activator occupying only the effector site and the substrate occupying only the active site was employed (Fig. 7). When no activator is present, only the enzyme substrate complex ES forms and leads to product. The model reduces to the simple Michaelis–Menten kinetics scheme:

$$E + S \underset{k_{-1}}{\overset{k_1}{\rightleftharpoons}} ES \xrightarrow{k_{cat}} E + P$$

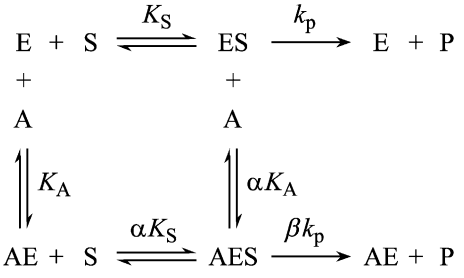

Fig. 7. The two-site kinetics model used to fit *L. monocytogenes* PI-PLC kinetics data with methyl-FLIP as the substrate. S, substrate; E, enzyme; A, activator; and P, product.

In the model of Fig. 7, quasi-equilibrium conditions are assumed. The observation of a moderate turnover number of 66 s^{-1} supports the use of this simplification. With this assumption, K_M becomes K_S and, by convention, $k_{cat}=k_p$. The notation adopted here is that of Segel [27], and the model is referred to as the 'mixed-type non-essential inhibition or activation' case (this is a technical definition—the activation is undoubtedly essential to the biological function). From thermodynamics, since formation of the complex AES can be carried out by two paths, there is an additional restraint that causes the symmetry in dissociation constants of Fig. 7. As the activator concentration is increased, the equilibrium shifts to the more productive AES complex. At an arbitrary concentration of A, product will be produced from both the upper and lower branches of the kinetic scheme in Fig. 7. The rate of the reaction is the sum of the rates of formation of product: $v=k_p[ES]+\beta k_p[AES]$. Eliminating the unknown [ES] and [AES] using the equilibrium expressions, and taking the ratio $v/[E]_T$ where $[E]_T$ is the total enzyme concentration, gives the final rate equation {Eq. (IV-23) or (V-2) in [27]}:

$$v=\frac{V_{max}\dfrac{[S]}{K_S}+\beta\ V_{max}\dfrac{[A][S]}{\alpha K_A K_S}}{1+\dfrac{[S]}{K_S}+\dfrac{[A]}{K_A}+\dfrac{[A][S]}{\alpha K_A K_S}} \quad (1)$$

where V_{max} is defined as the maximum rate in the *absence* of any activator: $V_{max}=k_p[E]_T$.

Without any loss of generality, Eq. (1) may be written in the more recognizable Michaelis–Menten equation form:

$$v=\frac{V_{max}^{app}[S]}{K_M^{app}+[S]} \quad (2)$$

The apparent Michaelis–Menten parameters K_M^{app} and V_{max}^{app} are given by:

$$K_M^{app}=K_S\frac{1+\dfrac{[A]}{K_A}}{1+\dfrac{[A]}{\alpha K_A}} \quad (3)$$

and

$$V_{max}^{app}=\frac{V_{max}\left(1+\dfrac{\beta[A]}{\alpha K_A}\right)}{1+\dfrac{[A]}{\alpha K_A}} \quad (4)$$

The K_M^{app} and V_{max}^{app} are constants only when [A] is held constant. Thus, the most useful case involves holding [A] fixed at an arbitrary value, while [S] is varied, as in the experiment of Fig. 6. We fitted the experimental data of Figs. 4 and 6 to the two-site model to find the parameters α and β. The quantities [A] and K_A associated with the activator are $[A]=[diC_6PC]=0.4$ mM and $K_A=K_d$ (determined from Fig. 5) $=0.06$ mM. The values of α and β calculated from Eq. (3) and Eq. (4) are $\alpha=0.33\pm0.04$ and $\beta=1.6\pm0.1$. The uncertainty in the parameter β was primarily due to the uncertainty in the measurement of V_{max}^{app}, and β was relatively insensitive to variations in K_A. For the purposes of this study, we did not obtain a second measurement of K_A by generating a family of curves as a function of varying concentrations of [A] using double reciprocal plots and secondary plots. In a study of an alkaline phosphatase in which K_A was measured from both the activation curve and from double reciprocal plots, the values were in agreement [28].

4. Discussion

L. monocytogenes PI-PLC catalyzes the cleavage of methyl-FLIP in the absence of any added lipid, and the behavior obeys Michaelis–Menten kinetics. The data are consistent with the fact that both enzyme and substrate are water-soluble monomers, and there are no complications from aggregation effects. Addition of short-chain zwitterionic lipid diC_6PC causes a sizable increase in activity. The concentrations of diC_6PC used are more than one order of magnitude below the critical micelle concentration (CMC) (15 mM) [29,30]. Thus, the activation is due to the binding of monomeric lipid to the enzyme. We do not rule out the possibility that the PI-PLC enzyme binds more than one diC_6PC below the CMC. It is known, for example,

that cobra venom phospholipase A_2 (PLA_2) acts as a nucleation site for the formation of microaggregates with diC_6PC and diC_7PC below the CMCs of the pure lipids [31,32]. Likewise, inhibition studies of pig and bovine pancreatic PLA_2 have been interpreted as indicating that aggregates of enzyme with short-chain anionic phospholipids occur below the CMC [33]. Compared to bacterial PI-PLCs, however, PLA_2 enzymes have a stronger affinity for organized lipid substrates, and the Ca^{2+} ions present for enzyme activity can facilitate microaggregation. A plausible model for the present case is that one diC_6PC molecule binds first to the monomeric PI-PLC at very low concentrations, followed by additional molecules as the onset of micelle formation is approached. Such intermediate clustering of diC_6PC could be less optimal for substrate binding and catalysis, and be responsible for the decrease in activation at diC_6PC concentrations above approximately 0.4 mM, as observed in Fig. 5. Assuming that the initial activation is due to binding of one lipid molecule, a fit to the first four data points in Fig. 5 yields an estimate of K_d (or K_A) $= 0.06 \pm 0.01$ mM. In comparison, NMR data on binding of the same lipid to *B. thuringiensis* PI-PLC indicate a single binding site, with $K_d = 0.5 \pm 0.2$ mM [34]. Thus, the *L. monocytogenes* PI-PLC and *B. thuringiensis* PI-PLC show similar diC_6PC binding behavior. Given the difficulties of these measurements, the different experimental conditions, and the fact that both the activation and NMR results are model-dependent, the differences in K_d may not be significant other than to suggest that the *L. monocytogenes* PI-PLC has a slightly higher affinity for diC_6PC than does *B. thuringiensis* PI-PLC.

When a fixed amount of diC_6PC is added, the initial rates of catalysis as a function of [S] are greater than the rates in the absence of the short-chain lipid. The shape of the rate vs. [S] curve remains hyperbolic. We can deduce, without any models, that there is activation by diC_6PC and that it reduces K_M and increases V_{max}. That is, activation results from a combination of increased affinity of the active site for the substrate and increased turnover number (k_{cat}). The data fit the two-site model of Fig. 7, yielding values for the two parameters α and β. The occupation of the activator site causes an increase in catalytic efficiency (k_{cat}/K_M), the size of which is given by dividing the $\beta k_p/\alpha K_S$ ratio in the presence of the activator (lower branch of Fig. 7) by the k_p/K_S ratio (or k_{cat}/K_M from the Michaelis–Menten equation) in the absence of the activator (upper branch of Fig. 7). This ratio reduces to $\beta/\alpha = 1.6/0.33 = 4.8$. This is the first quantitative study of *L. monocytogenes* PI-PLC kinetics and activation, but the general effect of activation by PC has previously been noted in studies of *B. cereus* PI-PLC and nearly identical *B. thuringiensis* PI-PLC [35,36]. In addition, the two-site model of Fig. 7 has previously been used to explain activation in the second reaction of *B. thuringiensis* PI-PLC, in which the enzyme slowly hydrolyzes the product of the first reaction, I(1,2)cP, to form *myo*-inositol 1-phosphate [37].

The activation step described in Fig. 7 is a classic, two-site interaction model. It is quite probable that this model describes an initial event occurring at low diC_6PC concentrations and is succeeded by lipid–protein interactions that, as additional lipid is added, result in subtle rearrangements of the contacts between protein and lipid, and expand to the interfacial interactions of a micellar complex above the CMC. The terms cooperativity or allostery are often used in describing such events [34,35,38], but the definition differs somewhat from that of classical enzymology. We discuss this point briefly here in the hope that it will help to minimize confusion. In a broad sense, cooperativity is used to describe many processes in chemistry, such as protein folding, DNA and RNA melting, other phase changes, monolayers (e.g. deviations from the Langmuir isotherm), in glasses, and in other situations where multiple weak interactions can combine to produce an effect greater than the sum of the individual interactions. Cooperativity is an anthropomorphic concept: two entities interact to produce a greater (or lesser) result [39]. The essence of cooperativity is a molecular event that depends on an event that has taken place previously (e.g. binding or conformational change, or fluctuation). In the specific area of multiple ligand binding, such as oxygen binding to hemoglobin, or in multimeric enzymes involved in metabolic control, the textbook defi-

nition is more restrictive: cooperativity in these cases is only applied to ligand binding to *identical* multiple sites. Positive cooperativity refers to situations where the site-specific binding constant K_{j+1} for the $j+1$ binding event is greater than K_j, and binding constants have been adjusted for any statistical effects [39–41]. Allostery refers to a substance causing a change by binding to the allosteric site, a site distinct from the active site (or ligand binding sites in proteins that are not enzymes, e.g. hemoglobin). The effects are usually propagated from one domain to another in a multimeric enzyme. The effects observed in phospholipases do not meet these strict enzymological definitions of cooperativity and allostery. The phospholipases in general are monomeric and have only one active site. There are many subsites, but these are not likely to be identical. Interactions between these subsites and multiple substrate molecules involve cooperativity and allostery (e.g. subsite occupation affects activity) under the broader definitions of these terms. The cause is likely to be small rearrangements in residues in the interfacial contact region of the enzyme. The situation is similar in the paradigm in enzymology, bovine pancreatic ribonuclease A (RNase A). RNase A is a small, monomeric enzyme with one active site, and yet the kinetic effects under certain conditions are ascribed to cooperativity [42]. RNase A has three nucleotide binding subsites and undergoes processivity, or one-dimensional diffusion along RNA, that is similar in concept to the two-dimensional scooting of phospholipases [43]. Cooperative effects are likely to occur whenever enzymes interact with polymeric substrates, e.g. DNA, RNA, polypeptides, polysaccharides or lipid membranes.

Acknowledgments

We thank Drs G. Bruce Birrell, Karen K. Hedberg and Irwin H. Segel for useful discussions. We also are pleased to acknowledge a debt of gratitude to our colleague Dr John A. Schellman for his valuable contributions to research and teaching of biophysical chemistry at the University of Oregon. This work was supported by NIH grants GM 25689, GM 27137 and AI-45153.

References

[1] M.L. Paul, D.E. Dwyer, C. Chow, et al., Listeriosis—a review of eighty-four cases, Med. J. Aust. 160 (1994) 489–493.

[2] Centers for Disease Control, Multistate outbreak of listeriosis—United States, MMWR Morb. Mortal. Wkly. Rep. 49 (2000) 1129–1130.

[3] D.A. Portnoy, T. Chakraborty, W. Goebel, P. Cossart, Molecular determinants of *Listeria monocytogenes* pathogenesis, Infect. Immun. 60 (1992) 1263–1267.

[4] G. Smith, H. Marquis, S. Jones, N. Johnston, D. Portnoy, H. Goldfine, The two distinct phospholipases C of *Listeria monocytogenes* have overlapping roles in escape from a vacuole and cell-to-cell spread, Infect. Immun. 63 (1995) 4231–4237.

[5] P. Glaser, L. Frangeul, C. Buchrieser, et al., Comparative genomics of *Listeria* species, Science 294 (2001) 849–852.

[6] T. Bannam, H. Goldfine, Mutagenesis of active-site histidines of *Listeria monocytogenes* phosphatidylinositol-specific phospholipase C: effects on enzyme activity and biological function, Infect. Immun. 67 (1999) 182–186.

[7] A. Camilli, L.G. Tilney, D.A. Portnoy, Dual roles of *plcA* in *Listeria monocytogenes* pathogenesis, Mol. Microbiol. 8 (1993) 143–157.

[8] O.H. Griffith, M. Ryan, Bacterial phosphatidylinositol-specific phospholipase C: structure, function, and interaction with lipids, Biochim. Biophys. Acta 1441 (1999) 237–254.

[9] D.W. Heinz, M. Ryan, T.L. Bullock, O.H. Griffith, Crystal structure of the phosphatidylinositol-specific phospholipase C from *Bacillus cereus* in complex with *myo*-inositol, EMBO J. 14 (1995) 3855–3863.

[10] D.W. Heinz, M. Ryan, M.P. Smith, L.H. Weaver, J.F.W. Keana, O.H. Griffith, Crystal structure of phosphatidylinositol-specific phospholipase C from *Bacillus cereus* in complex with glucosaminyl($\alpha 1 \rightarrow 6$)-D-*myo*-inositol, an essential fragment of GPI anchors, Biochemistry 35 (1996) 9496–9504.

[11] J. Moser, B. Gerstel, J.E. Meyer, T. Chakraborty, J. Wehland, D.W. Heinz, Crystal structure of the phosphatidylinositol-specific phospholipase C from the human pathogen *Listeria monocytogenes*, J. Mol. Biol. 273 (1997) 269–282.

[12] R.L. Williams, Mammalian phosphoinositide-specific phospholipase C, Biochim. Biophys. Acta 1441 (1999) 255–267.

[13] D.W. Heinz, L.O. Essen, R.L. Williams, Structural and mechanistic comparison of prokaryotic and eukaryotic phosphoinositide-specific phospholipases C, J. Mol. Biol. 275 (1998) 635–650.

[14] T.O. Zaikova, A.V. Rukavishnikov, G.B. Birrell, O.H. Griffith, J.F. Keana, Synthesis of fluorogenic substrates

for continuous assay of phosphatidylinositol-specific phospholipase C, Bioconjug. Chem. 12 (2001) 307–313.
[15] C.S. Gässler, M. Ryan, T. Liu, O.H. Griffith, D.W. Heinz, Probing the roles of active site residues in phosphatidylinositol-specific phospholipase C from *Bacillus cereus* by site-directed mutagenesis, Biochemistry 36 (1997) 12802–12813.
[16] J.A. Koke, M. Yang, D.J. Henner, J.J. Volwerk, O.H. Griffith, High-level expression in *Escherichia coli* and rapid purification of phosphatidylinositol-specific phospholipase C from *Bacillus cereus* and *Bacillus thuringiensis*, Protein Exp. Purif. 2 (1991) 51–58.
[17] B. Witholt, M. Boekhout, M. Brock, J. Kingma, H. Van Heerikhuizen, L. De Leij, An efficient and reproducible procedure for the formation of spheroplasts from variously grown *Escherichia coli*, Anal. Biochem. 74 (1976) 160–170.
[18] S.C. Gill, P.H. von Hippel, Calculation of protein extinction coefficients from amino acid sequence data, Anal. Biochem. 182 (1989) 319–326.
[19] O.H. Griffith, J.J. Volwerk, A. Kuppe, Phosphatidylinositol-specific phospholipases C from *Bacillus cereus* and *Bacillus thuringiensis*, Methods Enzymol. 197 (1991) 493–502.
[20] E.B. Cogan, G.B. Birrell, O.H. Griffith, A robotics-based automated assay for inorganic and organic phosphates, Anal. Biochem. 271 (1999) 29–35.
[21] M. Leimeister-Wächter, E. Domann, T. Chakraborty, Detection of a gene encoding a phosphatidylinositol-specific phospholipase C that is co-ordinately expressed with listeriolysin in *Listeria monocytogenes*, Mol. Microbiol. 5 (1991) 361–366.
[22] H. Goldfine, C. Knob, Purification and characterization of *Listeria monocytogenes* phosphatidylinositol-specific phospholipase C, Infect. Immun. 60 (1992) 4059–4067.
[23] H. Nielsen, J. Engelbrecht, S. Brunak, G. von Heijne, Identification of prokaryotic and eukaryotic signal peptides and prediction of their cleavage sites, Protein Eng. 10 (1997) 1–6.
[24] R. Taguchi, Y. Asahi, H. Ikezawa, Purification and properties of phosphatidylinositol-specific phospholipase C of *Bacillus thuringiensis*, Biochim. Biophys. Acta 619 (1980) 48–57.
[25] A.J. Leigh, J.J. Volwerk, O.H. Griffith, J.F. Keana, Substrate stereospecificity of phosphatidylinositol-specific phospholipase C from *Bacillus cereus* examined using the resolved enantiomers of synthetic *myo*-inositol 1-(4-nitrophenyl phosphate), Biochemistry 31 (1992) 8978–8983.
[26] K.A. Lewis, V.R. Garigapati, C. Zhou, M.F. Roberts, Substrate requirements of bacterial phosphatidylinositol-specific phospholipase C, Biochemistry 32 (1993) 8836–8841.
[27] I.H. Segel, Enzyme Kinetics: Behavior and Analysis of Rapid Equilibrium and Steady-State Enzyme Systems, John Wiley & Sons Inc, New York, 1975.
[28] M.L. Bonet, F.I. Llorca, E. Cadenas, Alkaline *p*-nitrophenylphosphate phosphatase activity from *Halobacterium halobium*. Selective activation by manganese and effect of other divalent cations, Int. J. Biochem. 24 (1992) 839–845.
[29] R.J.M. Tausk, J. Karmiggelt, C. Oudshoorn, J.T.G. Overbeek, Physical chemical studies of short-chain lecithin homologues. I. Influence of the chain length of the fatty acid ester and of electrolytes on the critical micelle concentration, Biophys. Chem. 1 (1974) 175–183.
[30] J. Bian, M.F. Roberts, Comparison of surface properties and thermodynamic behavior of lyso- and diacylphosphatidylcholines, J. Colloid Interface Sci. 153 (1992) 420–428.
[31] T. Bukowski, D.C. Teller, Self-association and active enzyme forms of *Naja naja naja* and *Crotalus atrox* phospholipase A_2 studied by analytical ultracentrifugation, Biochemistry 25 (1986) 8024–8033.
[32] J.H. van Eijk, H.M. Verheij, R. Dijkman, G.H. de Haas, Interaction of phospholipase A_2 from *Naja melanoleuca* snake venom with monomeric substrate analogs, Eur. J. Biochem. 132 (1983) 183–188.
[33] J. Rogers, B.Z. Yu, S.V. Serves, et al., Kinetic basis for the substrate specificity during hydrolysis of phospholipids by secreted phospholipase A_2, Biochemistry 35 (1996) 9375–9384.
[34] C. Zhou, X. Qian, M.F. Roberts, Allosteric activation of phosphatidylinositol-specific phospholipase C: specific phospholipid binding anchors the enzyme to the interface, Biochemistry 36 (1997) 10089–10097.
[35] J.J. Volwerk, E. Filthuth, O.H. Griffith, M.K. Jain, Phosphatidylinositol-specific phospholipase C from *Bacillus cereus* at the lipid–water interface: interfacial binding, catalysis, and activation, Biochemistry 33 (1994) 3464–3474.
[36] C. Zhou, Y. Wu, M.F. Roberts, Activation of phosphatidylinositol-specific phospholipase C toward inositol 1,2-(cyclic)-phosphate, Biochemistry 36 (1997) 347–355.
[37] C. Zhou, M.F. Roberts, Non-essential activation and competitive inhibition of bacterial phosphatidylinositol-specific phospholipase C by short-chain phospholipids and analogues, Biochemistry 37 (1998) 16430–16439.
[38] Y. Wu, O. Perisic, R.L. Williams, M. Katan, M.F. Roberts, Phosphoinositide-specific phospholipase C δ1 activity toward micellar substrates, inositol 1,2-cyclic phosphate, and other water-soluble substrates: a sequential mechanism and allosteric activation, Biochemistry 36 (1997) 11223–11233.
[39] I.M. Klotz, Ligand Receptor Energetics, John Wiley & Sons Inc, New York, 1997.
[40] E. Di Cera, Site-specific thermodynamics: understanding cooperativity in molecular recognition, Chem. Rev. 98 (1998) 1563–1592.

[41] S. Forsén, S. Linse, Cooperativity: over the Hill, Trends Biochem. Sci. 20 (1995) 495–497.
[42] M. Moussaoui, M.V. Nogués, A. Guasch, T. Barman, F. Travers, C.M. Cuchillo, The subsites structure of bovine pancreatic ribonuclease A accounts for the abnormal kinetic behavior with cytidine 2′,3′-cyclic phosphate, J. Biol. Chem. 273 (1998) 25565–25572.
[43] B.R. Kelemen, R.T. Raines, Extending the limits to enzymatic catalysis: diffusion of ribonuclease A in one dimension, Biochemistry 38 (1999) 5302–5307.